AERODYNAMIC CATEGORIZATION OF SPACECRAFT IN LOW EARTH ORBITS

Bent Fritsche

HTG – Hyperschall Technologie Göttingen GmbH
Albert-Einstein-Strasse 11
37191 Katlenburg-Lindau, Germany

ABSTRACT

Spacecraft re-entering the Earth atmosphere in an uncontrolled manner may get stabilised by restoring aerodynamic torques, if they have an appropriate shape and mass distribution. While the aerodynamic force (mainly drag) is usually a second-order effect compared to the gravitational acceleration by the Earth at altitudes above 150 km, the aerodynamic torques can compete with the Earth gravitation gradient-induced torques sometimes already at altitudes at and below 250 km. Therefore it is of interest to have an understanding of how to compute the aerodynamic torques in this altitude regime.

In this paper the theory of the computation of the aerodynamic coefficients at altitudes above 150 km, where the flow regime is free-molecular, is revisited and applied for simple geometric shapes as well as for a composite shape. The idea is to map eventually arbitrarily-shaped spacecraft onto simple geometric shapes to classify their aerodynamic attitude behavior by their coefficients.

Index Terms— Free-molecular flow, Aerodynamic coefficients, Analytical approach

1. INTRODUCTION

The usual approach to compute the aerodynamic coefficients at high altitudes is to construct a surface model of the spacecraft, where the surface is either modelled with plane face elements or discretized into small triangular or quadrangular ”panels”. The aerodynamic coefficients are then computed for each surface element and summed up with an Integral or Monte-Carlo method, utilizing that the flow around the spacecraft can be considered as free-molecular.

While the Monte-Carlo method can give quite accurate coefficients for a given configuration, it does not provide information on configuration changes. This is different to analytical solutions, where the geometric dimensions and mass distribution appear as explicit parameters, and where the influence of configuration changes on the results are obvious. On the other hand, the possibility to get analytical solutions is limited to convex geometric shapes. This can be extended to concave shapes by using some kind of shadowing algorithms, but in this case the additional effort needed to examine the shadowed areas can foil the advantages of the analytical approach compared to the numerical analysis.

In any case the combination of different methods can give an added value. For basic geometries analytical solutions are known. Comparing these solutions with Monte-Carlo results can serve as a calibration method for the Monte-Carlo method statistical uncertainties. For more complex geometries the Monte-Carlo method can give a measure of the effect of shadowing and multiple reflections, which cannot be considered exactly or not at all in analytical solutions or integral methods.

Due to the special form of the free-molecular gas-surface interaction and its momentum transfer some simplifications are possible especially for the typical high-speed conditions in orbit, which can be used to extend the validity of the analytical solutions or at least extend their approximate range of validity.

2. ANALYTICAL SOLUTIONS

2.1. Basic Equations

Aerodynamic forces and torques acting on a spacecraft are calculated by integrals over the spacecraft surface area A exposed to the flow:

$$\vec{F} = \int_A \vec{f}(\vec{r})\, dA \tag{1}$$

$$\vec{M} = \int_A (\vec{r} - \vec{r}_{cm}) \times \vec{f}(\vec{r})\, dA \tag{2}$$

where $\vec{f}(\vec{r})$ is the local aerodynamic stress (force per area), and $\vec{r}_{cm}$ is a moment reference point.

Eqns. (1) and (2) can be nondimensionalized by factoring out the dynamic free-stream pressure $q_\infty = \rho_\infty V_\infty^2/2$, where ρ_∞ and V_∞ are the free-stream density and velocity, and introducing reference values for area A_{ref} and length L_{ref}, and introducing local force coefficients $\vec{f}(\vec{r}) = q_\infty \vec{c}_f(\vec{r})$:

$$\vec{F} = q_\infty A_{ref} \vec{C}_F \tag{3}$$

$$\vec{M} = q_\infty A_{ref} L_{ref} \vec{C}_M \tag{4}$$

$$\vec{C}_F = \frac{1}{A_{ref}} \int_A \vec{c}_f(\vec{r})\, dA \tag{5}$$

$$\vec{C}_M = \frac{1}{A_{ref} L_{ref}} \int_A (\vec{r} - \vec{r}_{cm}) \times \vec{c}_f(\vec{r})\, dA \tag{6}$$

For trajectory and attitude propagation problems it is more convenient to use dimensional coefficients:

$$\vec{C}_{FA} = \int_A \vec{c}_f(\vec{r})\, dA \tag{7}$$

$$\vec{C}_{MV} = \int_A (\vec{r} - \vec{r}_{cm}) \times \vec{c}_f(\vec{r})\, dA \tag{8}$$

where the trailing letter in the subscript indicates, that the quantity is either an area (in $\vec{C}_{FA}$) or a volume (in $\vec{C}_{MV}$). The advantage of using dimensional coefficients is that there is no need for normalisation and denormalisation by reference quantities. Then,

$$\vec{F} = q_\infty \vec{C}_{FA} \quad (9)$$
$$\vec{M} = q_\infty \vec{C}_{MV} \quad (10)$$
$$\vec{C}_F = \frac{\vec{C}_{FA}}{A_{ref}} \quad (11)$$
$$\vec{C}_M = \frac{\vec{C}_{MV}}{A_{ref} L_{ref}} \quad (12)$$

The local force coefficient depends on the gas-surface interaction. Using the Maxwell model, where it is assumed that a fraction σ of the molecules impinging on the spacecraft surface is reflected diffusely and the remaining fraction $(1-\sigma)$ is reflected specularly, one gets

$$\begin{aligned}\vec{C}_F &= \frac{1}{A_{ref}} \int_A (\sigma\, \vec{c}_{f,diff}(\vec{r}) \\ &+ (1-\sigma)\, \vec{c}_{f,spec}(\vec{r}))\, dA \quad (13)\\ \vec{C}_M &= \frac{1}{A_{ref} L_{ref}} \int_A (\vec{r} - \vec{r}_{cm}) \times (\sigma\, \vec{c}_{f,diff}(\vec{r}) \\ &+ (1-\sigma)\, \vec{c}_{f,spec}(\vec{r}))\, dA \quad (14)\end{aligned}$$

with [1]

$$\begin{aligned}\vec{c}_{f,diff} &= -\frac{1}{\sqrt{\pi} S^2} \left(\Pi(S_n) + \frac{\sqrt{\pi}}{2} \sqrt{\frac{T_W}{T_\infty}} \chi(S_n) \right) \vec{n} \\ &+ \frac{S_t \chi(S_n)}{\sqrt{\pi} S^2}\, \vec{t} \quad (15)\\ \vec{c}_{f,spec} &= -\frac{2}{\sqrt{\pi S^2}} \Pi(S_n)\, \vec{n} \quad (16)\end{aligned}$$

where $\vec{n}$ and $\vec{t}$ are the normal and tangential surface unit vectors, S_n and S_t are the normal and tangential components of the speed ratio vector $\vec{S} = \vec{V}\sqrt{m/2kT_\infty}$, T_W and T_∞ are the temperature of the wall surface element and the temperature of the ambient atmosphere, and

$$\Pi(S_n) = S_n \mathrm{e}^{-S_n^2} + \sqrt{\pi}(S_n^2 + \frac{1}{2})(1 + \mathrm{erf}\,(S_n)) \quad (17)$$
$$\chi(S_n) = \mathrm{e}^{-S_n^2} + \sqrt{\pi} S_n (1 + \mathrm{erf}\,(S_n)) \quad (18)$$

While the surface normal unit vector $\vec{n}$ is defined locally by the surface geometry, the tangential unit vector depends also on the velocity direction:

$$\begin{aligned}\vec{t} &\sim (\vec{V} \times \vec{n}) \times \vec{n} \quad (19)\\ &= (\vec{n}\vec{V})\vec{n} - \vec{V} \quad (20)\\ \vec{t} &= (\vec{n}\cos\theta - \vec{v})/\sin\theta \quad (21)\end{aligned}$$

where θ is the angle between velocity and normal direction, and $\vec{v}$ is the unit velocity vector. With

$$S_n = S\cos\theta, \quad S_t = S\sin\theta \quad (22)$$

(15) can be expressed alternatively in the form

$$\begin{aligned}\vec{c}_{f,diff} &= -\frac{1}{2S^2} \left(1 + \mathrm{erf}\,(S\cos\theta) + \sqrt{\frac{T_W}{T_\infty}} \chi(S\cos\theta) \right) \vec{n} \\ &- \frac{\chi(S\cos\theta)}{\sqrt{\pi} S}\, \vec{v} \quad (23)\end{aligned}$$

defining three force coefficients:

$$\vec{c}_{f,diff} = (c_{n,i} + \sqrt{\frac{T_W}{T_\infty}} c_{n,r})\vec{n} + c_{v,i}\vec{v} \quad (24)$$

For a numerical computation of the aerodynamic coefficients the body's surface is partitioned into small surface elements, so that for each element the surface normal direction can be regarded as approximately constant. The integrals (13) and (14) are then approximated by sums over the contributions of each surface element, computed from (15) and (16).

In an analytical treatment analytical closed-form solutions are sought for the integrals (13) and (14), using (23) and (16) for the coefficients. Different to the numerical treatment, where only the values are needed for each surface element, in the analytical treatment the surface geometry is analyzed for possible simplifications, special cases and symmetries.

For the computation of the coefficients the vectors $\vec{n}$ and $\vec{v}$ have to be known. $\vec{n}$ is a function of the spacecraft geometry and can be expressed as function of the surface coordinate:

$$\vec{n} = (n_x(x,y,z), n_y(x,y,z), n_z(x,y,z)) \quad (25)$$

The velocity direction can be expressed by the aerodynamic angles of attack and side slip, α and β. Mathematically the aerodynamic attitude of a body can be described by a rotation about the body-fixed z-axis (yaw rotation) by an angle $-\beta$, followed by a rotation about the body-fixed y-axis (pitch rotation) by an angle α. This is equivalent to a pitch rotation about the body-fixed y-axis by angle α, followed by a yaw rotation about the space-fixed z-axis by angle $-\beta$. In both cases the components of the velocity vector in the body-fixed frame are

$$\vec{v} = (\cos\alpha\cos\beta, \sin\beta, \sin\alpha\cos\beta) \quad (26)$$

An alternative rotation sequence is a pitch rotation by the so-called total angle of attack about an axis which is in general neither aligned with a body-fixed axis nor a wind axis, and a roll angle about the body-fixed x-axis. The total angle of attack is uniquely defined as the angle between the body-fixed axis and the wind x-axis:

$$\cos\alpha_T = \cos\alpha\cos\beta \quad (27)$$

The roll angle ϕ can then be determined to be

$$\cot\phi = \sin\alpha\cot\beta \quad (28)$$

Then

$$\vec{v} = (\cos\alpha_T, \sin\alpha_T\sin\phi, \sin\alpha_T\cos\phi) \quad (29)$$

(29) is especially suited for geometries with rotational symmetry.

In the following sections formulas will be derived for the diffuse reflection part of the force and moment coefficients. According to [2] it is a reasonable assumption, that the gas-surface interaction is completely diffuse ($\sigma = 1$) at least for flight altitudes below 300 km. In this case the following considerations are similar to Sentman's derivations [3].

For ease of formulation the suffix diffuse will be omitted. Referring to (23) following notation will be used:

$$\begin{aligned}\vec{c}_f &= -\frac{1}{2S^2} \left(1 + \mathrm{erf}\,(S_n) + \sqrt{\frac{T_W}{T_\infty}} \chi(S_n) \right) \vec{n} \\ &- \frac{\chi(S_n)}{\sqrt{\pi} S}\, \vec{v} \quad (30)\\ &= (c_{n,i}\vec{n} + c_{v,i}\,\vec{v}) + \sqrt{\frac{T_W}{T_\infty}} c_{n,r}\vec{n} \quad (31)\\ &= \vec{c}_{f,i} + \sqrt{\frac{T_W}{T_\infty}} \vec{c}_{f,r} \quad (32)\end{aligned}$$

Figure 1 shows the factors in the local coefficients which are dependent on the normal coefficient of the speed ratio S_n.

$1+\text{ erf }(S_n)$ appears only in $c_{n,i}$. It is bounded by the values 0 and 2. Since there is an additional factor proportional to $1/S^2$ in this coefficient, this means that at hypersonic speeds ($S > 5$) the contribution of the incident molecules to the normal component in (30) will be generally small. It has to be noted, however, that there is another contribution in the normal direction by the incident molecules by the normal component of the velocity.

The function $\chi(S_n)$ appears in the contribution of the incident molecules in the direction of the velocity $c_{v,i}$ as well as in the contribution of the reflected molecules in normal direction $c_{n,r}$. This function is less than 1 on the leeside ($S_n < 0$), but rises linearly with S_n already at supersonic normal speed ratios ($S_n > 1$). This means, that at low to moderate local inclination angle θ the contribution of the incident molecules in velocity direction $c_{v,i}$ becomes independent of the speed ratio, and only a function of θ. Compared to this the contribution of the reflected molecules in normal direction $c_{n,r}$, which has the same dependence on S_n, is approximately smaller by a factor of $\sqrt{T_W/T_\infty}/S$.

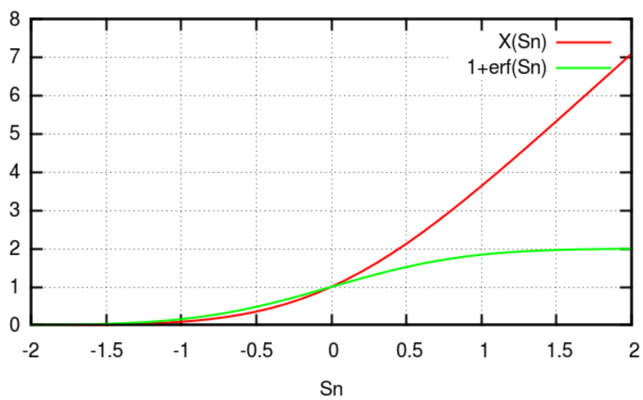

Fig. 1. S_n-dependence of the local coeffcients

2.2. Flat face

The simplest body of finite size is a single-sided flat face. While single-sided faces are physically not realistic, they are a helpful concept when constructing body surfaces from flat faces, where the face backsides are not visible from outside and do not have to be considered in the calculation of the outer surface coefficients.

2.2.1. Forces

For a flat face the force coefficient is constant over the whole surface, therefore the total force coefficient is just the local coefficient multiplied the surface area of the flat face A_{FF}

$$\vec{C}_{FA,FF} = \int_A \vec{c}_f dA = \vec{c}_f A_{FF} \tag{33}$$

The local force coefficient is given by (30), with

$$\vec{c}_{f,i} = -\frac{1}{2S^2}(1+\text{ erf }(S_n))\,\vec{n} - \frac{1}{\sqrt{\pi}S}\chi(S_n)\,\vec{v} \tag{34}$$

$$\vec{c}_{f,r} = -\frac{1}{2S^2}\chi(S_n)\,\vec{n} \tag{35}$$

As an example, a flat face with its surface aligned parallel to the y-z-plane, $\vec{n} = (1,0,0)$, $S_n = S_x$, and

$$\begin{aligned} \vec{C}_{FA,FF,i} &= -A_{FF}\left(\frac{1}{2S^2}(1+\text{ erf }(S_x))\,\vec{e}_x \right. \\ &+ \left. \frac{1}{\sqrt{\pi}S}\chi(S_x)\,\vec{v}\right) \end{aligned} \tag{36}$$

$$\vec{C}_{FA,FF,r} = -A_{FF}\frac{1}{2S^2}\chi(S_x)\,\vec{e}_x \tag{37}$$

with

$$S_x = S\cos\alpha\cos\beta \tag{38}$$

$$= S\cos\alpha_T \tag{39}$$

From (39) it is clear that the normal component of the speed ratio depends only on the total angle of attack, which is in the case of the flat face identical to the local flow inclination. This means, that the magnitudes of the coefficients for the flat face depend only on the total angle of attack.

Figure 2 shows the force coefficients of a flat face as function of angle of attack.

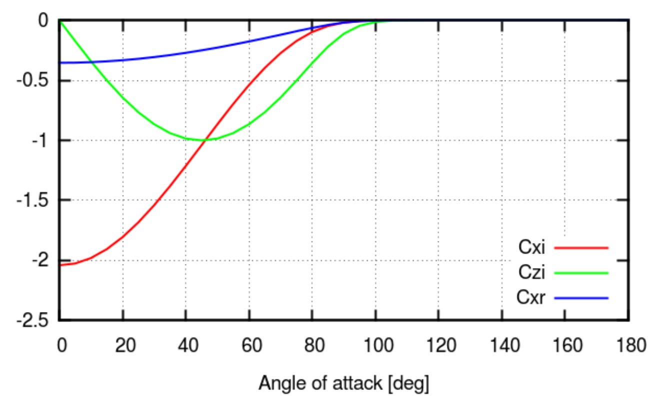

Fig. 2. Flat face force coefficients. The reference area is 1.

2.2.2. Moments

For a constant c_f (8) can be rewritten as

$$\vec{C}_{MV} = \int(\vec{r}\times\vec{c}_f)dA - \int(\vec{r}_{cm}\times\vec{c}_f)dA \tag{40}$$

$$= \left(\int\vec{r}dA\right)\times\vec{c}_f - (\vec{r}_{cm}\times\vec{c}_f)A \tag{41}$$

$$= (\vec{r}_P - \vec{r}_{cm})\times\vec{C}_{FA} \tag{42}$$

where the notation $\vec{r}_P = (\int\vec{r}dA)/A$ was used. By definition, r_P is identical to the center of area of the face. With (42) the moment acting on a flat face can be computed from the total force coefficient:

$$\vec{C}_{MV,FF} = (\vec{r}_{P,FF} - \vec{r}_{cm})\times\vec{C}_{FA,FF} \tag{43}$$

The moment reference point $\vec{r}_{cm}$ can be located everywhere, therefore no flat face tag was added to it. For the special case $r_{cm} = r_{P,FF}$, for example, it follows immediately that the moment about the center of area of the face is zero, regardless of the magnitude of the force acting on it.

2.3. Flat plate

A flat plate will be regarded here as a double-sided flat face. This is a more physical realistic type of shape, except that its thickness is assumed to be zero.

2.3.1. Forces

For a flat plate, the force coefficients of a flat face have to computed for both sides and then added. Both sides differ in the direction of their normals: they are oppositely directed. This means, that in the coefficient equations $\vec{n}$ changes sign for the opposite face, but also S_n. Summing up both contributions gives for the force coefficients of a flat plate

$$\vec{c}_{f,i} = -\frac{1}{S^2} \text{ erf } (S_n)\,\vec{n} - \frac{1}{\sqrt{\pi}S}\chi_+(S_n)\,\vec{v} \tag{44}$$

$$\vec{c}_{f,r} = -\frac{1}{2S^2}\chi_-(S_n)\,\vec{n} \tag{45}$$

with the definitions

$$\chi_+(S_n) = \chi(S_n) + \chi(-S_n) \tag{46}$$

$$= 2\exp(-S_n^2) + 2\sqrt{\pi}S_n \text{ erf } (S_n) \tag{47}$$

$$\chi_-(S_n) = \chi(S_n) - \chi(-S_n) \tag{48}$$

$$= 2\sqrt{\pi}S_n \tag{49}$$

The functions $\chi_+(S_n)$ and $\chi_-(S_n)$ are shown in Figure 3.

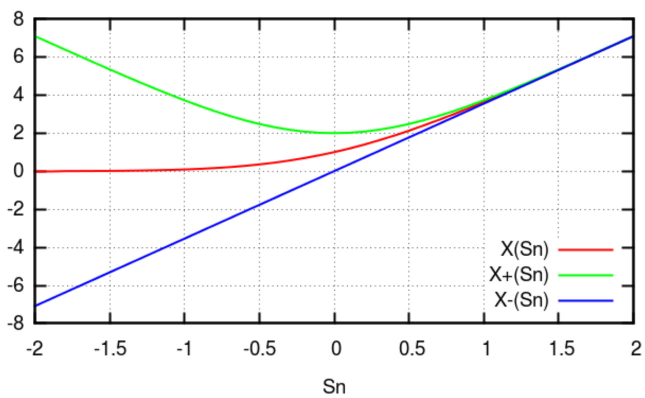

Fig. 3. Functions χ, χ_+, and χ_-

The total force coefficients is given by (33):

$$\vec{C}_{FA,FP,i} = -A_{FP}\left(\frac{1}{S^2} \text{ erf } (S_n)\,\vec{n} + \frac{1}{\sqrt{\pi}S}\chi_+(S_n)\,\vec{v}\right) \tag{50}$$

$$\vec{C}_{FA,FP,r} = -A_{FP}(\frac{1}{2S^2}\chi_-(S_n)\,\vec{n}) \tag{51}$$

Figure 4 shows the force coefficients of a flat face as function of angle of attack.

2.3.2. Moments

Since for a flat plate the center of areas concide for both faces, (42) can be applied here as well, using for $\vec{C}_F$ the total force coefficient of the plate:

$$\vec{C}_{MV,FP} = (\vec{r}_{P,FP} - \vec{r}_{cm}) \times \vec{C}_{FA,FP} \tag{52}$$

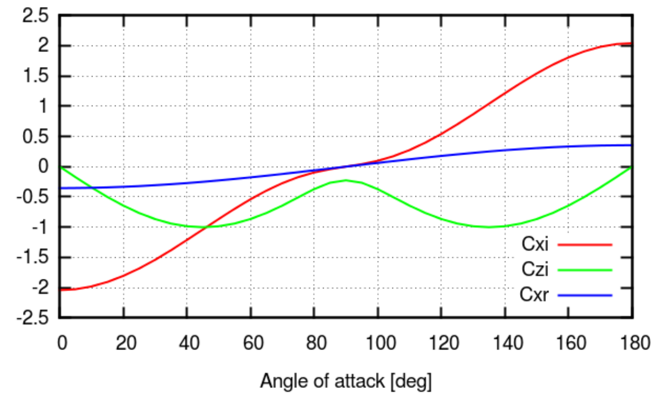

Fig. 4. Flat plate force coefficients. The reference area is 1.

2.4. Box

Flat face and flat plate are defined by their normal direction and surface area. In the following all shapes will be regarded as centered and aligned w.r.t. a geometric coordinate system. Actually this assumption does not reduce the generality of the results, but gives the possibility to be more specific in the values.

A box will be defined here as a rectangular body with given size in x, y, and z-direction and centered around the geometric coordinate origin. The sizes are called length l, width w, and height h.

2.4.1. Forces

For a box we have three pairs of oppositely oriented faces. Different to a flat plate they have also different locations.

For the x-faces, $\vec{n} = (\pm1, 0, 0)$, $\vec{n}\vec{v} = \pm v_x$, for the y-faces, $\vec{n} = (0, \pm1, 0)$, $\vec{n}\vec{v} = \pm v_y$, for the z-faces, $\vec{n} = (0, 0, \pm1)$, $\vec{n}\vec{v} = \pm v_z$. Inserting into (50) and (51) and summing up yields

$$\vec{C}_{FA,B,i} = -\frac{1}{S^2}(\text{ erf } (S_x)A_x\vec{e}_x + \text{ erf } (S_y)A_y\vec{e}_y + \text{ erf } (S_z)A_z\vec{e}_z) - \frac{1}{\sqrt{\pi}S}(\chi_+(S_x)A_x + \chi_+(S_y)A_y + \chi_+(S_z)A_z)\,\vec{v} \tag{53}$$

$$\vec{C}_{FA,B,r} = -\frac{\sqrt{\pi}}{S}(A_x v_x\vec{e}_x + A_y v_y\vec{e}_y + A_z v_z\vec{e}_x) \tag{54}$$

The flat plate formulas could be used since the force coefficients only depend on the normal vectors of the different planes, not on their position.

Figure 5 shows the force coefficients of a box as function of angle of attack.

2.4.2. Moments

For the moment coefficients the face positions become relevant since they determine the lever arm. Therefore we have to refer to the flat face formulas. In doing so it makes sense to split up the contributions of the face centers (due to the $\vec{r}_P$s) and the reference point offset $\vec{r}_{cm}$.

For a box $\vec{r}_P$ has the same direction as $\vec{n}$ for each face. Therefore the $\vec{n}$-component of the force coefficients does not contribute to the moments. This means in particular that the reflected molecules do

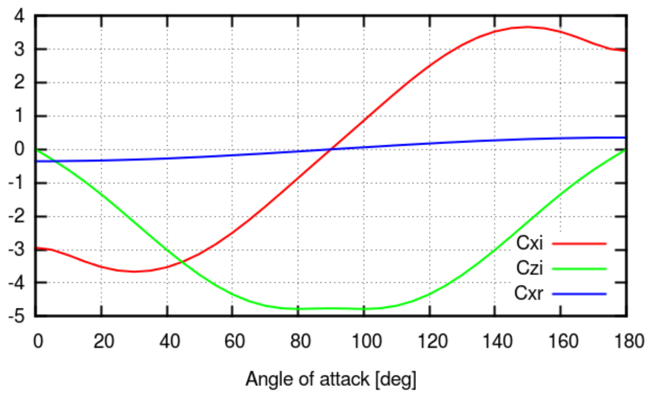

Fig. 5. Box force coefficients. The box dimensions are $l = 2$, $w = 1$, $h = 1$. The reference area is 1.

not contribute to the moments at all. For the incident molecules

$$\vec{C}_{MV,B,i} = \sum_{i=1}^{6} \vec{r}_P \times C_{F,i} \quad (55)$$

$$= -\frac{1}{\sqrt{\pi}S}\left(\chi_-(S_x)\frac{A_x l}{2}\vec{e}_x + \chi_-(S_y)\frac{A_y w}{2}\vec{e}_y + \chi_-(S_z)\frac{A_z h}{2}\vec{e}_z\right) \times \vec{v} \quad (56)$$

$$= -\frac{V}{S}\vec{S} \times \vec{v} \quad (57)$$

$$= 0 \quad (58)$$

$$\vec{C}_{MV,B,r} = 0 \quad (59)$$

where $V = A_x l = A_y w = A_z h$ denotes the box volume. This means that a box has no moment w.r.t. its geometric center. So for the total moment of a box

$$\vec{C}_{MV,B} = \vec{r}_{cm} \times (\vec{C}_{FA,B,i} + \vec{C}_{FA,B,r}) \quad (60)$$

2.5. Circular cylinder

2.5.1. Forces

Mantle

The local normal vector is

$$\vec{n} = \cos\phi\,\vec{e}_y + \sin\phi\,\vec{e}_z \quad (61)$$

and

$$\vec{C}_{FA,CC,m,i} = -Rl\left(\frac{1}{2S^2}\int_0^{2\pi}(1 + \text{ erf }(S_y\cos\phi + S_z\sin\phi))(\cos\phi\vec{e}_y + \sin\phi\vec{e}_z)\,d\phi + \frac{1}{\sqrt{\pi}S}\vec{v}\int_0^{2\pi}\chi(S_y\cos\phi + S_z\sin\phi)\,d\phi\right) \quad (62)$$

$$\vec{C}_{FA,CC,m,r} = -Rl\frac{1}{2S^2}\int_0^{2\pi}\chi(S_y\cos\phi + S_z\sin\phi)(\cos\phi\vec{e}_y + \sin\phi\vec{e}_z)\,d\phi \quad (63)$$

The calculation of these coefficients requires the computation of several integrals which are functions of two parameters (S_y and S_z). Due to the special form of the integrals it appears possible to translate them into a one-parameter form, which simplifies their evaluation. Defining $S_{yz} = \sqrt{S_y^2 + S_z^2}$, the integrals can be re-written as

$$\vec{C}_{FA,CC,m,i} = -Rl\left(\frac{1}{2S^2}\int_0^{2\pi}(1 + \text{ erf }(S_{yz}\sin(\phi + \phi_0)))(\cos\phi\vec{e}_y + \sin\phi\vec{e}_z)\,d\phi + \frac{1}{\sqrt{\pi}S}\vec{v}\int_0^{2\pi}\chi(S_{yz}\sin(\phi + \phi_0))\,d\phi\right) \quad (64)$$

$$\vec{C}_{FA,CC,m,r} = -Rl\frac{1}{2S^2}\int_0^{2\pi}\chi(S_{yz}\sin(\phi + \phi_0))(\cos\phi\vec{e}_y + \sin\phi\vec{e}_z)\,d\phi \quad (65)$$

with $\phi_0 = \arccos(S_z/S_{yz}) = \arcsin(S_y/S_{yz})$. With the redefinition $\phi \to \phi + \phi_0$:

$$\vec{C}_{FA,CC,m,i} = -Rl\left(\frac{1}{2S^2}\int_0^{2\pi}(1 + \text{ erf }(S_{yz}\sin\phi))(\cos(\phi - \phi_0)\vec{e}_y + \sin(\phi - \phi_0)\vec{e}_z)\,d\phi + \frac{1}{\sqrt{\pi}S}\vec{v}\int_0^{2\pi}\chi(S_{yz}\sin\phi)\,d\phi\right) \quad (66)$$

$$= -Rl\left(\frac{1}{2S^2}\int_0^{2\pi}(1 + \text{ erf }(S_{yz}\sin\phi))((\cos\phi\cos\phi_0 + \sin\phi\sin\phi_0)\vec{e}_y + (\sin\phi\cos\phi_0 - \cos\phi\sin\phi_0)\vec{e}_z)d\phi + \frac{1}{\sqrt{\pi}S}\vec{v}\int_0^{2\pi}\chi(S_{yz}\sin\phi)\,d\phi\right) \quad (67)$$

$$\vec{C}_{FA,CC,m,r} = -Rl\frac{1}{2S^2}\int_0^{2\pi}\chi(S_{yz}\sin\phi)(\cos(\phi - \phi_0)\vec{e}_y + \sin(\phi - \phi_0)\vec{e}_z)\,d\phi \quad (68)$$

$$= -Rl\frac{1}{2S^2}\int_0^{2\pi}\chi(S_{yz}\sin\phi)(\cos\phi\cos\phi_0 + \sin\phi\sin\phi_0)\vec{e}_y + (\sin\phi\cos\phi_0 - \cos\phi\sin\phi_0)\vec{e}_z)d\phi \quad (69)$$

Using the identities

$$\int_0^{2\pi}\sin\phi\,d\phi = 0 \quad (70)$$

$$\int_0^{2\pi}\cos\phi\,d\phi = 0 \quad (71)$$

$$\int_0^{2\pi}\text{ erf }(x\sin\phi)\cos\phi\,d\phi = 0 \quad (72)$$

$$\int_0^{2\pi}\chi(x\sin\phi)\sin\phi\,d\phi = \pi^{3/2}x \quad (73)$$

$$\int_0^{2\pi}\chi(x\sin\phi)\cos\phi\,d\phi = 0 \quad (74)$$

$$(75)$$

and naming the remaining irreducible integrals as

$$I_1(x) = \int_0^{2\pi}\text{ erf }(x\,\sin\phi)\sin\phi d\phi \quad (76)$$

$$I_2(x) = \int_0^{2\pi}\chi(x\,\sin\phi)d\phi \quad (77)$$

Eqns. (67) and (69) can be expressed in the form

$$\vec{C}_{FA,CC,m,i} = -Rl\left((\sin\phi_0\vec{e}_y + \cos\phi_0\vec{e}_z)\frac{1}{2S^2}I_1(S_{yz}) + \frac{1}{\sqrt{\pi}S}\vec{v}\,I_2(S_{yz})\right) \quad (78)$$

$$\vec{C}_{FA,CC,m,r} = -Rl(\sin\phi_0\vec{e}_y + \cos\phi_0\vec{e}_z)\frac{1}{2S^2}\pi^{3/2}S_{yz} \quad (79)$$

In cartesian coordinates this gives

$$\vec{C}_{FA,CC,m,i,x} = -Rl\frac{1}{\sqrt{\pi}S}\cos\alpha_T I_2(S\sin\alpha_T) \quad (80)$$

$$\vec{C}_{FA,CC,m,i,y} = -Rl\sin\phi_0\left(\frac{1}{2S^2}I_1(S\sin\alpha_T) + \frac{1}{\sqrt{\pi}S}\sin\alpha_T I_2(S\sin\alpha_T)\right) \quad (81)$$

$$\vec{C}_{FA,CC,m,i,z} = -Rl\cos\phi_0\left(\frac{1}{2S^2}I_1(S\sin\alpha_T) + \frac{1}{\sqrt{\pi}S}\sin\alpha_T I_2(S\sin\alpha_T)\right) \quad (82)$$

The integrals I_1 and I_2 are non-standard mathematical functions, but they are well-behaved, and they could be considered as defined by these definitions. It is possible to express these functions by modified Bessel functions, but this is not considered here, since the modified Bessel functions do not have the desired asymptotic behaviour for small and large arguments x.

End faces

$$\vec{C}_{FA,CC,e,i} = -A_e\left(\frac{1}{S^2}\,\mathrm{erf}\,(S_x)\,\vec{e}_x + \frac{1}{\sqrt{\pi}S}\chi_+(S_x)\,\vec{v}\right) \quad (83)$$

$$\vec{C}_{FA,CC,e,r} = -A_e\frac{\sqrt{\pi}}{S}\,\vec{e}_x \quad (84)$$

where $A_e = \pi R^2$ is the end face area.

Figure 6 shows the force coefficients of a cylinder as function of angle of attack.

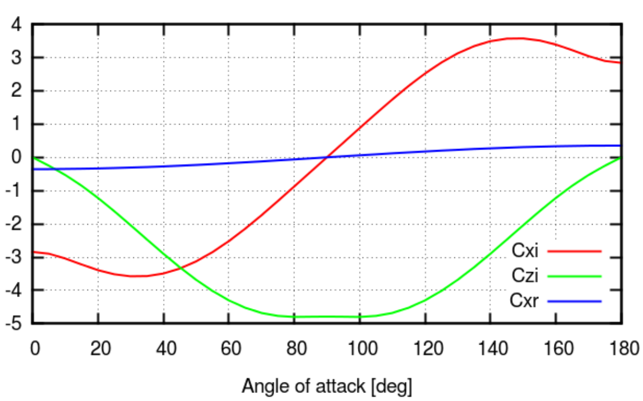

Fig. 6. Cylinder force coefficients. The cylinder dimensions are: $l = 2$, $r = 1/\sqrt{\pi}$. The reference area is 1.

2.5.2. *Moments*

Mantle

$$\vec{C}_{MV,CC,m,i} = -\frac{R^2 l}{\sqrt{\pi}S}\int_0^{2\pi}\vec{n}\times\chi(S_y\cos\phi + S_z\sin\phi)\vec{v}\,d\phi \quad (85)$$

$$= -\frac{R^2 l}{\sqrt{\pi}S}\left(\int_0^{2\pi}\chi(S_y\cos\phi + S_z\sin\phi)(\cos\phi\,\vec{e}_y + \sin\phi\,\vec{e}_z)\,d\phi\right)\times\vec{v} \quad (86)$$

With the same substitutions as applied for the force coefficients the integral can be reformulated

$$\vec{C}_{MV,CC,m,i} = -R^2 l\frac{1}{\sqrt{\pi}S}\left(\int_0^{2\pi}\chi\,d\phi(S_{yz}\sin\phi)\,(\cos\phi\cos\phi_0 + \sin\phi\sin\phi_0)\vec{e}_y \quad (87)\right.$$

$$\left. + (\sin\phi\cos\phi_0 - \cos\phi\sin\phi_0)\vec{e}_z)\right)\times\vec{v} \quad (88)$$

which finally gives, using (73) and (74)

$$\vec{C}_{MV,CC,m,i} = -\frac{R^2 l}{\sqrt{\pi}S}\left(\pi^{3/2}S_{yz}(\sin\phi_0\vec{e}_y + \cos\phi_0\vec{e}_z)\right)\times\vec{v} \quad (89)$$

$$= -\pi R^2 l\sin\alpha_T(\sin\phi_0\vec{e}_y + \cos\phi_0\vec{e}_z)\times\vec{v} \quad (90)$$

$$= -\pi R^2 l\sin\alpha_T\cos\alpha_T(\cos\phi_0\vec{e}_y - \sin\phi_0\vec{e}_z) \quad (91)$$

End faces

$$\vec{C}_{MV,CC,e,i} = -\pi R^2 l\cos\alpha_T\sin\alpha_T(-\cos\phi_0\vec{e}_y + \sin\phi_0\vec{e}_z) \quad (92)$$

Total

The total moment coefficients are then again zero in the symmetric case ($r_{cm} = 0$)

$$\vec{C}_{MV,CC,i} = \vec{C}_{MV,CC,m,i} + \vec{C}_{MV,CC,e,i} \quad (93)$$

$$= 0 \quad (94)$$

$$\vec{C}_{MV,CC,r} = 0 \quad (95)$$

In the general case,

$$\vec{C}_{MV,CC} = \vec{r}_{cm}\times(\vec{C}_{FA,CC,i} + \vec{C}_{FA,CC,r}) \quad (96)$$

3. APPLICATION TO A REAL SATELLITE

As an application case of the analytical approach the GOCE satellite will be used. For this satellite a surface panel model had been created earlier with the ANGARA software [4]. With this software the free-molecular aerodynamic and the solar radiation pressure induced force and torque coefficients can be calculated for arbitrarily shaped spacecraft. Figure 7 shows a view of the GOCE panel model.

The shape of the satellite consists essentially of an octacon-shaped main body in x-direction (front/back) with wings in z-direction (down/up) and flaps in y-direction (below/above) in the back.

For an analytical approach it seems reasonable at first to construct a simplified model consisting of a cylindrical main body with two flat plates modelling the wings. The problem with such a model is that one will get strong effects by shadowing and multiple reflections, which cannot be considered in the analytical approach, at least not in an easy way.

The results of the analytical considerations in the previous sections show, that for hypersonic speeds the local aerodynamic coefficients are mainly directed in velocity direction and therefore the

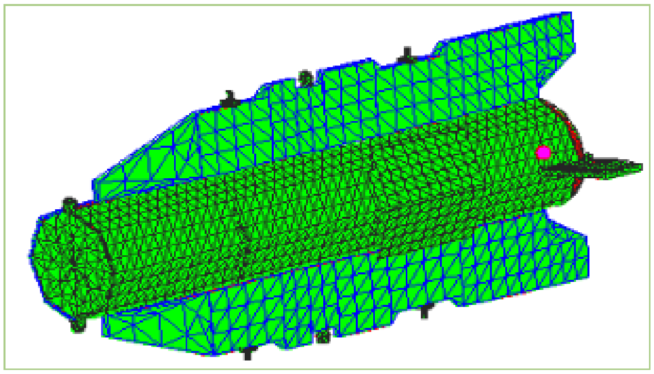

Fig. 7. GOCE surface panel model

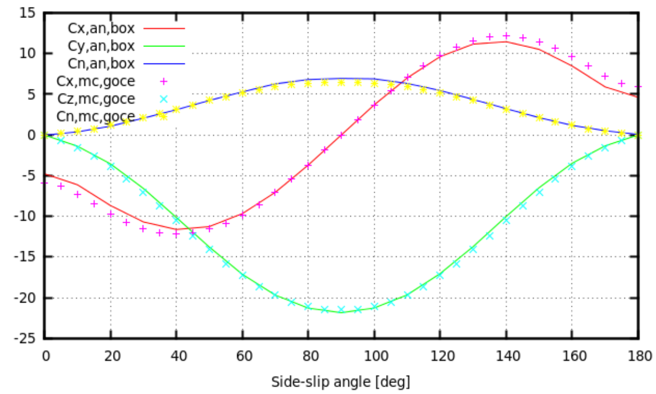

Fig. 9. Aerodynamic coefficients of GOCE, computed with the Monte-Carlo method, compared with a similar-sized "equivalent box", computed analytically, as function of angle of side slip (no angle of attack)

projected area is of major importance. So it appears reasonable to approximate the GOCE satellite just by a box with appropriately selected dimensions. An added value is that one gets automatically rid of shadowing and multiple reflection problems.

In the following the aerodynamic coefficients of the complete GOCE model as computed with the ANGARA software will be compared with the corresponding coefficients of a simple box with roughly similar overall dimensions as computed with an analytical formula (cf. Sec.2.4). The selected dimensions were: length $l = 5$ m, width $w = 0.7$ m, height $h = 2$ m. Compared are only the contributions of the incident molecules.

Figure 8 shows the results of the computation of the axial and normal force coefficients C_x and C_z as well as of the pitching moment C_m for GOCE and for the box as function of angle of attack (no side-slip).

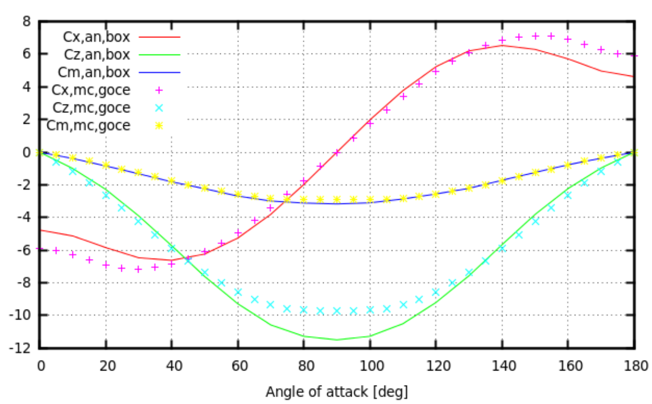

Fig. 8. Aerodynamic coefficients of GOCE, computed with the Monte-Carlo method, compared with a similar-sized "equivalent box", computed analytically, as function of angle of attack (no side-slip)

Figure 9 shows the results of the computation of the axial and side-force force coefficients C_x and C_y as well as of the yawing moment C_n for GOCE and for the box as function of side-slip angle (no angle of attack).

4. CONCLUSIONS

In this paper analytical solutions for the aerodynamic coefficients of simple-shaped bodies in free-molecular flow have been derived. The approach used differs from previous approaches in the use of a more symbolic notation, which makes it possible to find more compact expressions for the coefficients, and a different consideration of normal and tangential components.

The advantage of a more manageable form of the coefficients is the possible application to real satellites. This was demonstrated in the paper for the GOCE satellite, where with a simple surrogate box model the coefficents of the full model calculated by a Monte-Carlo method could be quite accurately reproduced by an analytical calculation. This could be a first step to classify the aerodynamic properties of arbitrarily-shaped spacecraft by mapping them onto simple geometric shapes.

5. REFERENCES

[1] Koppenwallner, G., "Freimolekulare Aerodynamik für Satellitenanwendung", DFVLR-FB 82-08, 1982.

[2] Moe, K., and Moe M.M., "Gas-surface interactions and satellite drag coefficients", Planetary and Space Science, 53, 793-801, 2005.

[3] Sentman, Lee H., "Free molecule flow theory and its application to the determination of aerodynamic forces", LMSC-448514, Lockheed Missiles Space Company, 1961.

[4] Fritsche, B., Ivanov, M., Kashkovsky, A., Koppenwallner, G., Kudryavtsev, A., Voskoboinikov, U., and Zhukova, G., "Radiation pressure forces on complex spacecraft", Final report, ESOC contract 11908/96/D/IM, HTG, Germany, 1998.